

## Influence of two-stage aeration on short-course simultaneous nitrification and denitrification of aerobic granular sludge

Wenxiao Wang, Wei Bian, Jun Li\*, Qing Zhao, Dongbo Liang, Yiqi Sun

National Engineering Laboratory for Advanced Municipal Wastewater Treatment and Reuse Technology, Engineering Research Center of Beijing, Beijing University of Technology, Beijing 100124, China, Tel. +8613691022490, email: 464078588@qq.com (W. Wang), Tel. +8615811418433, email: yangzhoubw@163.com (W. Bian), Tel. +8613611249208, email: bjutlijun@126.com (J. Li), Tel. +8617710664450, email: 374343833@qq.com (Q. Zhao), Tel. +8617710664450, email: 1144736849@qq.com (D. Liang), Tel. +8617710664450, email: 1037902374@qq.com (Y. Sun)

Received 14 September 2017; Accepted 23 March 2018

### ABSTRACT

The two-stage aeration operational mode was used in an aerobic granular sludge (AGS) sequencing batch reactor, under different high and low aeration time distribution. Obtained results showed that the introduction of the low aeration stage provided a good denitrification environment, alleviating the competition for nutrients between heterotrophic aerobic microorganisms. This method had quickly realized the process of short range simultaneous nitrification and denitrification (SSND), the total nitrogen removal rate increased from 40% to about 75%. The ratio of PN/PS rose from 1.27 to the highest value of 1.81, which improved the mass transfer efficiency in a single particle and enhanced the stability of AGS. Furthermore, it was known from the results of confocal laser scanning microscope (CLSM) and high-throughput pyrosequencing and phylogenetic assignment that the nitrite-oxidizing bacteria (NOB) were not completely washed, but rather stored in dead cells, in the inner layer of AGS. Consequently, this method could save the energy needed for aeration and improve the nitrogen removal performance and stability of AGS.

*Keywords:* Two-stage aeration; Short-range simultaneous nitrification and denitrification; Microbiological analysis; Confocal laser scanning microscope

### 1. Introduction

Aerobic granular sludge (AGS) aggregates with numerous types of strains that are embedded in a matrix of extracellular polymeric substances (EPS), inorganic compounds and various minerals. Compared to the activated sludge process, AGS has high biomass retention, good settling property and efficient nutrient removal, in a single reactor [1–3]. AGS has a hierarchical structure, which forms anoxic and anaerobic zones in the micro-environment of a single particle, achieving simultaneous nitrification and denitrification (SND) [4]. However, in the operation of a conventional AGS reactor, nitrogen removal under aerobic conditions is not sufficiently high

and the stability is very poor, which limited the development of granular sludge [5].

EPS, secreted by microbes during growth and lysis [6], which could maintain the structure of the granules [7] and contribute to sludge stability. Proteins (PN) and polysaccharides (PS) are the main components of EPS, containing multiple functional groups, which could change the sludge surface properties and hydrophobic forces. In addition, For AGS, a slight change in the concentration of DO led to a change in the EPS value, causing the stability of the granular sludge to be damaged. For example, a previous study reported that granular sludge developed at 100% saturation became unstable when oxygen saturation was decreased to 40% [8]. However, high aeration may not be a necessary condition for sludge granulation [9]. Wan and colleagues

\*Corresponding author.

[10] successfully developed AGS at DO values close to 2 mg/L (25% saturation) by adding nitrate to the system, thus, stable aerobic granular sludge can also be produced under moderate DO conditions. In that sense, granular sludge formation could benefit from SND, which is commonly observed in the granulation process [11]. Under the low concentration of DO, the SND process was easier to be realized, therefore, the low concentration of DO was beneficial to the stable operation of AGS. Additionally, some studies had shown that high aeration is beneficial to the formation of granular sludge. On the one hand, high aeration could reduce the mass transfer resistance between media, increasing the transfer efficiency of nutrients and oxygen between the water and the sludge [12]. On the other hand, the high shear force could promote the secretion of extracellular polymers, and appropriate hydraulic shear force was necessary to maintain the stable operation of AGS [13]. In summary, under appropriate conditions, AGS could be operated steadily regardless of the high dissolved oxygen concentration or low dissolved oxygen concentration, and enhanced performance in many aspects.

In this study, a two-stage aeration mode was employed. First, low aeration was used to stabilize the DO at about 0–2 mg/L, thereby increasing the denitrification efficiency and enhancing the denitrification capacity. Subsequently, aeration was increased to 5–7 mg/L, to improve the overall nitrification performance and maintain particle stability. The impact of micro-organisms, EPS level and other aspects of the two-stage aeration on the granular sludge was analyzed, aiming to make a theoretical contribution to the process of AGS denitrification.

## 2. Materials and methods

### 2.1. Reactor set-up

The AGS sequencing batch reactor (AGSBR) experimental device was shown in Fig. 1. The reactor was made of plexiglass, with an effective volume of 6 L, bottom diameter of 16 cm and a height of 32 cm. The inlet was equipped with an inlet pump, whereas the outlet allowed water flow by gravity. The air diffuser was designed at the bottom of the reactor, through the air pump for aeration, with an air flow meter that can be used to adjust the amount of aeration. Externally, the reactor also has an outfall, with the effluent ratio of 60%, which means that the volume of discharged water accounted for 60% of the total volume. In addition, the reactor was equipped with pH and DO on-line monitoring equipment that can display and record using the WTW instrument. The pH of the reactor was not controlled, whereas the pH value of the effluent was maintained between 7.5 and 7.9. Inoculated AGS is the result of a long-term SBR laboratory operation, and the obtained sludge had a concentration of 4000 mg/L, with a mixed liquor volatile suspended solids/mixed liquor suspended solids (MLVSS/MLSS) ratio of approximately 0.7, average particle size of about 3 mm and good settling performance.

The reactor was operated with a fixed cycle time of 12 h. The experiment was divided into 3 parts that were performed in parallel, R1: the low aeration time was 1 h, and

the high aeration time was 11 h; R2: the low aeration time was 2 h, and the high aeration time was 10 h; R3: the low aeration time was 3 h, and the high aeration time was 9 h. When the low aeration time was 4 h, and the high aeration time was 8 h, after the reactor had been running for 15 cycles, the disintegration of AGS appeared, and the denitrification performance decreased greatly, so we stopped the operation of the reactor.

The AGS was fed with synthetic wastewater, which contained approximately 300 mg COD/L, added as  $\text{CH}_3\text{COONa}$ ; 100 mg  $\text{NH}_4^+\text{-N/L}$ , added as  $\text{NH}_4\text{Cl}$ ; 3 mg P/L, added as  $\text{KH}_2\text{PO}_4$ , the concentration of  $\text{CaCl}_2\cdot 2\text{H}_2\text{O}$  was 100–120 mg/L and  $\text{MgSO}_4\cdot 7\text{H}_2\text{O}$  was 180–200 mg/L. Additionally,  $\text{NaHCO}_3$  was added to maintain alkalinity.

### 2.2. Analytical methods

All samples were filtered with a 0.45  $\mu\text{m}$  filter prior to the analysis.  $\text{NH}_4^+\text{-N}$ ,  $\text{NO}_2^-\text{-N}$ ,  $\text{NO}_3^-\text{-N}$ , MLSS and MLVSS were measured according to standard methods [14]. The average particle size was measured by laser particle size analyzer. The sludge microstructure and morphology were examined by scanning electron microscopy (SEM). Fluorescence *in situ* hybridization (FISH) was employed to determine the composition of the sludge. Samples were pretreated, then fixed and hybridized, as reported by Aoi et al. [15]. The probes used in the present study included EUB338, for the detection of most bacteria, NSO190, for ammonia oxidizing bacteria (AOB), Nit3, for nitrite oxidizing bacteria (NOB), fluorescein isothiocyanate (FITC), for extracellular proteins, Hoechst 33342, for live bacteria, and propidium iodide (PI), for dead bacteria (Table 1). Treated samples were detected by a confocal laser scanning microscope (CLSM; 156 Olympus FV1000, Japan). EPS extraction was performed as previously described [16,17]. Moreover, the determination of PN was based on the Bradford assay [18], whereas PS were determined using the anthrone-sulfuric acid colorimetric assay [19]. Besides, the particle size of the granular sludge used in the experiment was large and the internal structure was mature, the boundary between the inner layer and the outer layer was very obvious, so the outer part and the deep color inner part can be easily stripped.

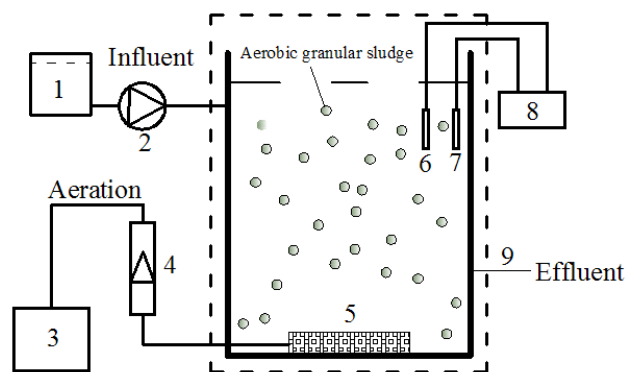


Fig. 1. Aerobic granular sludge Sequencing Batch Reactor: (1) Influent tank; (2) inlet pump; (3) Air pump; (4) Air flow meter; (5) Air diffuser; (6) Dissolved oxygen electrode; (7) pH electrode; (8) WTW monitor; (9) outfall.

### 2.3. Calculations

AGS (3500 mg/L) with pH of 7.5~8.0, was submitted to a small test (Fig. 2), at the temperature of 23°C. Due to AGS adsorption, SND, COD adsorption and the removal process being very short, liquid samples for testing were taken every 5 min in the first 30 min of the small test, to calculate the removal rates of COD, NO<sub>2</sub><sup>-</sup>-N, NO<sub>3</sub><sup>-</sup>-N (VrCOD, VrNO<sub>2</sub><sup>-</sup>-N, VrNO<sub>3</sub><sup>-</sup>-N) and the adsorption rate (Vads) by test data. The small test device is shown below, whereas the conditions of the small test are shown in Table 2.

According to the law of conservation of mass [20], the incoming COD was considered to be transformed into three fractions: COD adsorbed into biomass, oxidized COD and residual soluble COD in the outlet:

$$\text{COD}_{\text{inlet}} = \text{COD}_{\text{adsorpted}} + \text{COD}_{\text{oxidised}} + \text{COD}_{\text{outlet}} \quad (1)$$

Table 1  
Information relevant to FISH and dyes

Probes and dyes	Sequence (5'-3')	Specificity
EUB338	GCTGCCTCCCGTAGGAGT	Most bacteria
NSO190	CGATCCCCTGCTTTTCTCC	Ammonia-oxidizing b-Proteobacteria
NIT3	CCTGTGCTCCATGCTCCG	Nitrobacter spp.
FIYC	–	Extracellular protein
Hoechst 33342	–	live bacteria
PI	–	dead bacteria

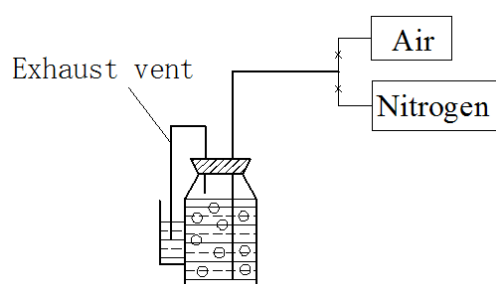


Fig. 2. small test device diagram.

Table 2  
small test conditions

Number	Wastewater conditions	Inflatable type	Measurable data
1	300 mg COD/L;	Air	VrCOD
2	300 mg COD/L;	Nitrogen	Vads
3	300 mg COD/L; 60 mg NO <sub>2</sub> <sup>-</sup> -N/L	Nitrogen	VrNO <sub>2</sub> <sup>-</sup> -N
4	300 mg COD/L; 60 mg NO <sub>3</sub> <sup>-</sup> -N/L	Nitrogen	VrNO <sub>3</sub> <sup>-</sup> -N

COD was supposed to be oxidized under anoxic or aerobic conditions:

$$\text{COD}_{\text{oxidatised}} = \text{COD}_{\text{anoxic}} + \text{COD}_{\text{aerobic}} \quad (2)$$

According to the small experiment and formulas (1) and (2), the rate of denitrification could be calculated using COD.

Nitrogen components were supposed to be transformed *via* assimilation by biomass, nitrification and denitrification. Hence, overall nitrogen balance becomes:

$$\text{N-NH}_{4\text{inlet}} + \text{N-NO}_{\text{xinlet}} = \text{N}_{\text{gas}} + \text{N-NO}_{\text{xoutlet}} + \text{N}_{\text{assimilation}} + \text{N-NH}_{4\text{outlet}} \quad (3)$$

The N<sub>assimilation</sub> value was considered negligible. Consequently, in this experiment, the total nitrogen removal rate can be calculated from Eq. (3):

$$R_{\text{TN}} = \{1 - [\text{N-NH}_{4\text{outlet}} + \text{N-NO}_{\text{xoutlet}}] / [\text{N-NH}_{4\text{inlet}} + \text{N-NO}_{\text{xinlet}}]\} \times 100 \quad (4)$$

### 2.4. Microbial sampling and phylogenetic assignment

In this study, AGS had a larger particle size and the gap between the inner and outer layers was noticeable, meaning that the outer layer (light color) could be easily separated from the inner layer (deep color) through artificial means. After taking the AGS out of the reactor, we rinsed the AGS 3–5 times with PBS buffer, then soak the AGS in PBS buffer and shake the particles for about 5 min, at this point, AGS structure was relatively loose, we could break the particle by the knife and tweezers, the inner and outer layers of AGS could be separated.

DNA was extracted from each sample according to a previously published method [21]. The extracted DNA was used for high-throughput pyrosequencing and phylogenetic assignment (Sangon, China).

## 3. Results and discussions

### 3.1. Effect of two-stage aeration of AGS on nitrogen removal

#### 3.1.1. Analysis of ammonia oxidation

According to Fig. 3, it can be seen that the effluent ammonia nitrogen concentration was basically 0 mg/L, meaning that the ammonia nitrogen removal was approximately 100%. Moreover, the increase in low aeration time led to a decrease in nitrification rate, which indicates that the high and low aeration time allocation has some effect on ammonia nitrogen removal. Additionally, the system had stable nitrification overall, in spite of the nitrification activity being inhibited in the low aeration stage. This might be because the long-term presence of nitrifying bacteria in the system was advantageous, although inhibited in hypoxic sections, nitrifying bacteria can rapidly recover their activity in the late high aerobic section. We can see from Fig. 4 that the introduction of low aeration stage was beneficial to the formation of anoxic environment, and which had little influence on aerobic nitrification process. As the low aeration stage created an almost anoxic environment, the outer

aerobic bacteria (aerobic heterotrophic bacteria and nitrifying bacteria) were inhibited to a certain extent, whereas denitrifying bacteria in the internal hypoxic areas could use sufficient carbon sources. Fig. 4 shows the organic concentration curve, which was detected in the typical cycle of three stages, after entering the high aeration stage, COD was reduced, causing the inhibition of outer heterotrophic bacteria, and thereby ensuring the activity of nitrifying bacteria.

### 3.1.2. Analysis of nitrogen accumulation

As seen in Fig. 5, the two-stage aeration method caused the nitrite accumulation rate increased significantly, from about 5% to about 85.34%. With the low aeration time lengthened, the nitrite accumulation rate also increased to a certain degree. This may be because the introduction of the low aeration stage caused a high amount of COD to be used in the denitrification. In the high aeration stage, COD was completely consumed and the DO concentration was high, as we can know that from Fig. 4, which inhibited the internal hypoxia of the AGS, basically stopping the denitrification process, which ultimately led to the accumulation of NO<sub>2</sub><sup>-</sup>-N. Due to the limitation of DO concentration, nitrification occurs mainly in the high aeration stage. Moreover, with the increase in the duration of the low

aeration stage, it is possible to shorten of the overall nitrification time during a 12 h cycle, which may be favorable for the accumulation of nitrogen. Since the autotrophic nitrifying bacteria in the reaction system are mainly AOB and NOB, and the rate of specific growth is mainly affected by microbial intrinsic parameters and substrate concentration, which is consistent with the two-factor limited Monod equation [22,23], the rate of specific growth of AOB and NOB bacteria was deduced by the formula:

$$\mu_x = \mu_{x,max} \left( \frac{S_x}{K_x + S_x} \right) \left( \frac{\rho_{DO}}{K_{DO} + \rho_{DO}} \right) \quad (5)$$

In Eq. (5),  $\mu_x$  was the specific growth rate of nitrifying bacteria (AOB or NOB), d<sup>-1</sup>;  $\mu_{x,max}$  was the maximum specific growth rate of nitrifying bacteria, d<sup>-1</sup>;  $S_x$  was the concentration of NH<sub>4</sub><sup>+</sup>-N or NO<sub>2</sub><sup>-</sup>-N, mg/L;  $K_x$  was the saturated constant of the substrate, mg/L;  $K_{DO}$  was the saturated constant of dissolved oxygen, mg/L; and  $\rho_{DO}$  was the concentration of dissolved oxygen in the reactor, mg/L.

As evidenced by Eq. (5), when the concentration of NH<sub>4</sub><sup>+</sup>-N is higher than  $K_x$ ,  $\mu_{AOB}$  mainly depends on the value of  $\rho_{DO}$ , and when  $\rho_{DO}$  (about 2 mg/L) >  $K_{DO}$ ,  $\mu_{AOB}$  reached the maximum. Due to the SND process, the concentration of NO<sub>2</sub><sup>-</sup>-N in the initial reaction was very low, that is,  $S_x$  was almost zero, and AOB had a small oxygen saturation constant (0.3 mg/L), whereas NOB had a large oxygen saturation constant (1.1 mg/L) [24] leading to  $\mu_{AOB} > \mu_{NOB}$ . In the entire reaction system, AOB achieved a greater degree of advantage (AOB activity increased), whereas NOB was at a disadvantage (NOB activity was inhibited). At the same time, the SND process reduced nitrate nitrogen to nitrite nitrogen, which led to the rapid nitrite accumulation. When the low aeration time was increased, resulting in a greater advantage of AOB, the accumulation of nitrous oxide was further enhanced.

### 3.1.3. Analysis of denitrification performance

After 60 days of culture, the three reactors were basically stable and the relevant data were measured. The denitrification performance parameters of AGSBR are listed in Table 3. The total nitrogen removal rate of the three reactors increased to different degrees, and the total nitrogen removal rate of R2 was the highest, increasing from

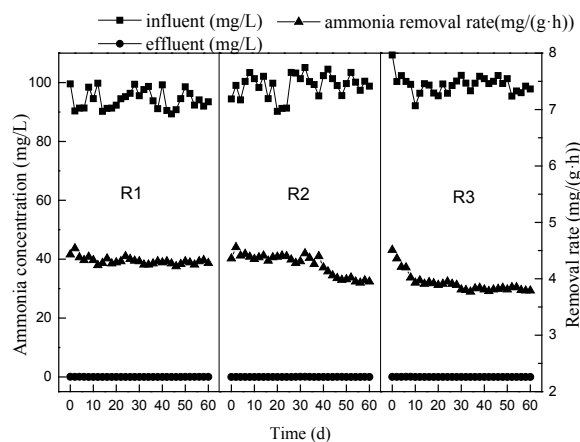


Fig. 3. Effect of high and low aeration time distribution on ammonia oxidation performance NH<sub>4</sub><sup>+</sup>-N.

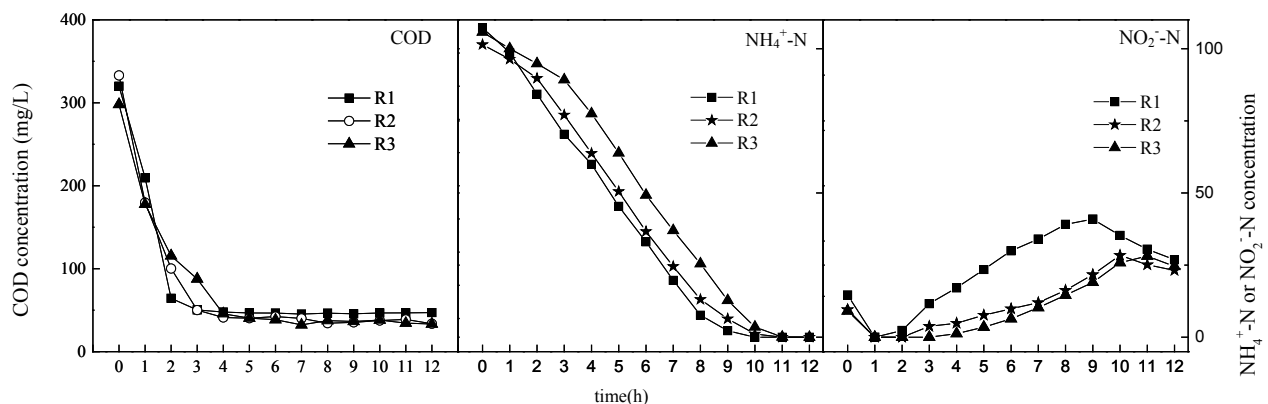


Fig. 4. The concentration curves of COD, NH<sub>4</sub><sup>+</sup>-N and NO<sub>2</sub><sup>-</sup>-N in a typical period.



about 40% to about 75%, visibly improving the denitrification performance. This can be explained by the fact that the low aeration stage creates a better denitrification environment, resulting in a significant increase in the activity of denitrifying microorganisms in the granular anoxic zone. Furthermore, even on the surface of the particles, the low aeration stage facilitates the use of sufficient carbon sources for denitrification, forming an adequate carbon storage for the high aeration stage, to ensure the stability of the denitrification [25]. The denitrification rate of nitrite in the three reaction systems was the most significant, and the rate ( $V_r\text{NO}_2^- \text{-N}$ ) of R2 was increased from about 1.45 mg/(gLVSS·h) to about 10.03 mg/(gLVSS·h), whereas the denitrification rate of  $\text{NO}_3^- \text{-N}$  in R1–R3 was only slightly increased, which indicated that the main denitrification process in the system was short-range denitrification. This could be because the concentration of  $\text{NO}_2^- \text{-N}$  in the system, which is the main substrate of denitrification, is high, and, therefore, the denitrification rate is greatly improved. It is noteworthy that the removal rate of total nitrogen did not increase with the increase in low aeration time, which may be because of the decrease in the rate of ammonia oxidation in the low aeration stage, resulting in a limited

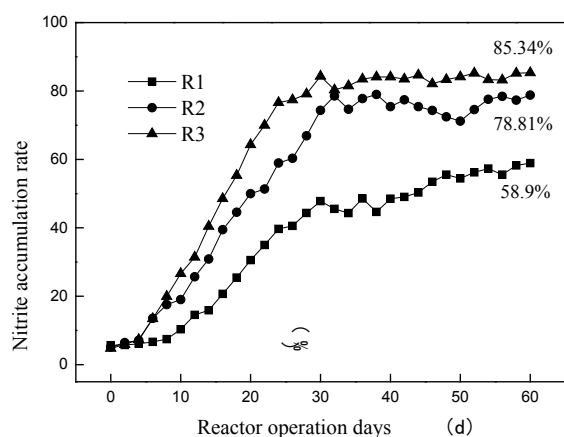


Fig. 5. Curve of the influence of the distribution of high and low aeration time on the accumulation rate of nitrogen.

concentration of nitrogen and a decrease in total nitrogen removal rate. Compared with other stages, R2 had the highest removal rate of TN and  $\text{NO}_2^- \text{-N}$ , which had the highest efficiency, and R2 had lower risk of particle instability than R3

### 3.2. Effect of two-stage aeration on microorganisms in AGS

#### 3.2.1. Analysis of the changes of EPS in AGS

Numerous reports have shown that EPS plays a significant role in the stability of AGS [26,27]. In this experiment, we mainly considered the PN and PS concentrations in EPS, and it can be seen from Table 3 that, through the culture of two-stage aeration, the PN/PS value was improved, which led to better hydrophobicity of the particles, thus improving the integrity of the granular sludge. Results revealed that, with the increase of EPS, the particle size was also obviously improved. Two-stage aeration may stimulate the microbial secretion of EPS, so that small particles can be more easily combined to form large particles, which leads to a larger zone for internal aerobic denitrification and provides a relatively stable structure. By artificially stripping the particles, we preliminarily explored the EPS values on the inside and outside of the particles in the R2 and the initial culture stage. Obtained results show that the PS value of the outside was higher than the inside, and the PS value was essentially unchanged overall. However the PN value of the outside was significantly higher than the initial culture stage, which shows that the outer microbes secreted numerous PN during the operation, which resulted in the increase of particle size and improved stability of the particles. In many studies, PN acts as a vehicle for the transport of substances between cells, increasing the ability of the cells to acquire energy and nutrients. The increase in PN also further improves the mass transfer efficiency of nutrients. Similar conclusions were drawn by means of 3D fluorescent staining (Fig. 6) of PN, which showed that the outside PN value was higher than in the inner layer. After two-stage aeration mode of culture, PN value was significantly improved in AGS, helping maintain the stability and mass transfer of particles, which ensured that the area of the anoxic zone increased in the high hydraulic shear.

Table 3  
Experimental data

Data	R1		R2		R3	
	Initial	Stable	Initial	Stable	Initial	Stable
$V_r\text{NO}_2^- \text{-N}^a$	1.39±0.35	7.35±0.23	1.45±0.15	10.03±0.21	1.13±0.22	8.92±0.11
$V_r\text{NO}_3^- \text{-N}^a$	0.78±0.21	2.48±0.09	0.88±0.12	3.39±0.33	1.01±0.38	3.27±0.27
$R_{\text{TN}} (\%)$	37.32	64.89	40.44	75.51	39.42	70.21
PN <sup>b</sup>	89.43±2.27	148.65±5.34	94.78±4.78	175.47±6.88	88.57±4.73	170.54±9.45
PS <sup>b</sup>	67.89±5.71	94.47±8.91	70.11±9.42	99.48±3.61	69.81±7.81	94.38±2.32
PN/PS	1.32	1.57	1.35	1.76	1.27	1.81
Size (mm)	2.94±0.54	4.02±1.02	3.07±0.99	4.97±0.65	3.02±0.44	5.14±0.76
VSS/SS	4000/2800	4520/3100	4600/3200	5150/3600	5200/3600	6150/4300

<sup>a</sup> $V_r\text{NO}_2^- \text{-N}$  and  $V_r\text{NO}_3^- \text{-N}$  unit were mg/(gLVSS·h).

<sup>b</sup>PS and PN unit were (mg/g LVSS)

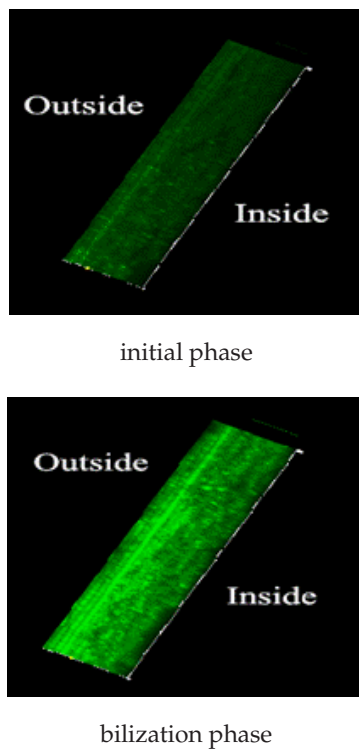


Fig. 6. 3D fluorescence picture of extracellular protein (The detection thickness is about 180  $\mu\text{m}$ ).

3.2.2. Analysis of microbial community change of AOB and NOB in AGS

The AGS of the initial stage and the R2 stabilization phase were tested by FISH, following the separation of the inside and outside of the granules by artificial means. The resulting fluorescence images are presented in Fig. 7, which shows that the number of bacteria outside was higher than the inside. This could be because the 3D structure of the granular sludge causes a certain degree of mass transfer resistance, and the inner layer was mainly composed of holes, which are formed by cell endogenous respiration and autolysis [28]. FISH images were roughly analyzed using a counting software (Image-Pro Plus 5.1, Media Cybernetics, USA). The ratio of the number of outer AOB to the total number of bacteria increased from about 1.3% to about 3.5%, whereas the proportion of NOB was almost unchanged, accounting for only 1% of the total bacteria. This result confirms that the specific growth rate of AOB was higher than NOB, to the advantage of nitrifying bacteria. The number of bacteria in the inside was significantly improved, but the proportion of AOB was very small (only about 1%), which shows that AOB (autotrophic aerobic microorganisms) were basically distributed on the surface of the aerobic layer, and rarely inside. It is worth noting that NOB was distributed inside of AGS, when NOB are at a disadvantage for a long time, they might lose their activity and became stored inside the particles.

The AGS was treated by the similar method and directly stained for live and dead cells using fluorescent dyes (Fig. 8). The obtained image shows that the number of living cells

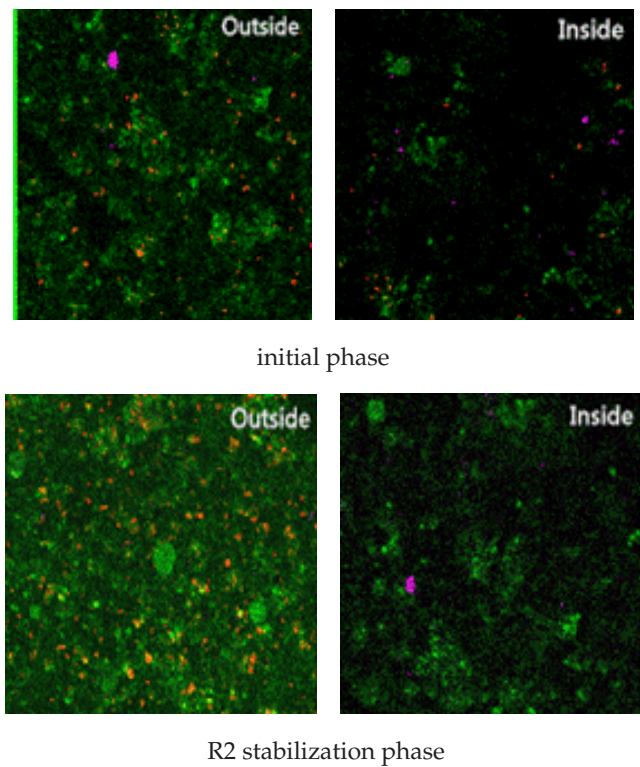


Fig. 7. FISH picture of AGS (Green represents the total bacteria, red represents AOB bacteria, and purple represents NOB bacteria).

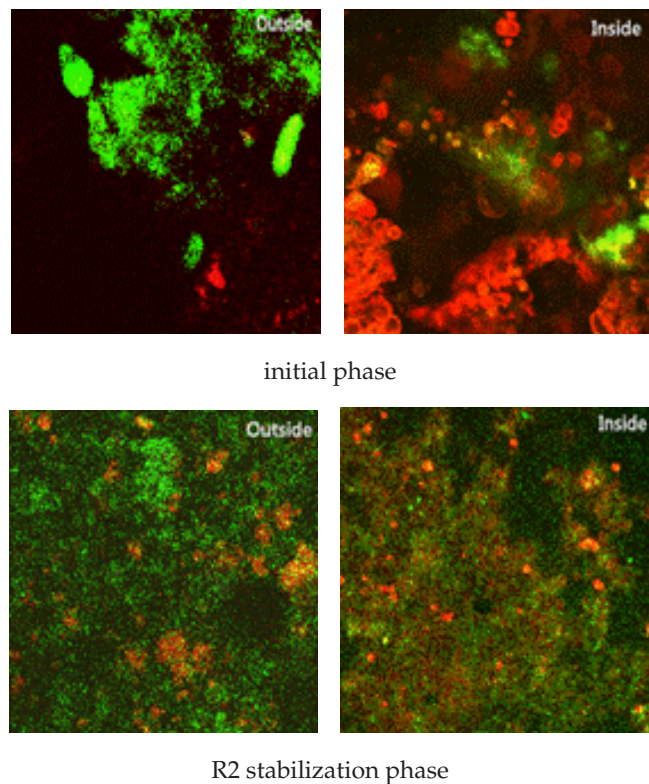


Fig. 8. Fluorescence picture of AGS (Green represents the living cells, red represents dead cells).

in the outside was greater than the number of cells inside, at any phase. The ratio of the inner cells to the total cells (the sum of the live and dead cells) increased from about 21.3–47.2%, indicating that the two-stage aeration method increased the particle size, but the mass transfer efficiency inside the particles was not significantly affected. Due to the PN increase between and in the cells, the transfer efficiency of nutrients was improved in AGS, which ensured the proper functioning of the inner cells.

### 3.2.3. Analysis of microbial community change of AGS

Sludge samples from the initial phase (number 1) and R2 stabilization phase were analyzed through high-throughput pyrosequencing, to estimate changes in microorganism. Sludge samples from the R2 stabilization phase were cut into outer sludge (number 2) and inner sludge (number 3) by artificial method. As seen in Fig. 9, the biological diversity of AGS was improved by the two-stage aeration operation. All three samples contained a large number of Proteobacteria and Bacteroidetes bacteria. Planctomycetes was a type of microbial species involved in anaerobic denitrification [29]. Their proportion of the total bacteria increased from the original 2.78–17.70% (outside 0.47%, inside 17.24%), which increased the internal anaerobic zone, providing a good anaerobic denitrification environment and resulting in the rapid proliferation of

microorganisms, ultimately improving the denitrification capacity. At the same time, it could be seen that AGS has the potential to remove hydrocarbons.

In domestic wastewater treatment, AOB mainly belong to the genera *Nitrosomonas* and *Nitrospira*, whereas NOB mainly belong to the genera *Nitrobacter* and *Nitrospira* [30]. Moreover, the genera *Paracoccus* and *Thauera* are known as common denitrifying bacteria [31,32]. *Nitrosospira* and *Nitrospira* were not detected in this study, and the four genera that were present in the total bacteria are listed in Table 4. After the two-stage aeration operation, the number of AOB and NOB increased from 0.33% and 0.28% to 4.45% and 0.55%, respectively, which confirmed the previous analysis of nitrification performance. The introduction of the low aeration stage, reduced the AOB, NOB and heterotrophic competition for nutrients, while sustaining the growth of AOB, which resulted in the AOB/NOB increase, the ratio is from the initial 1.2 to 8.1, ensuring the stability of nitrification and rapid realization of short-range nitrification. It is worth noting that there was a significant difference in the number of NOB in the outer and inner layers of AGS in R2. Considering the information in Fig. 6, it may be that NOB was not washed out of the system, but rather stored in dead cells in the AGS inner layer, becoming a part of the internal nucleus structure.

As the number of denitrifying bacteria was greatly improved, there was a large number of denitrifying bacteria in the outer layer of AGS, which may imply that the outer layer also had an oxygen-deficient zone in the low aeration stage, mainly due to the low aeration and high aeration stages using a carbon source for denitrification. Consequently, due to AGS mass transfer resistance in the inner layer, nutrient transport rate was slow, mainly in the low and high aeration stages of denitrification.

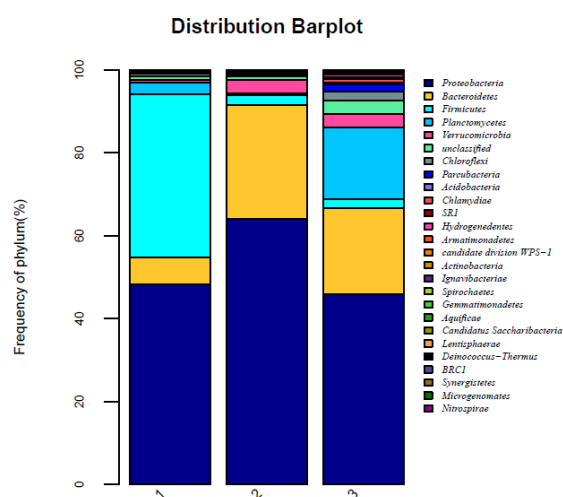


Fig. 9. Microbial community composition at the phylum level of the AGS, based on the 16S rRNA gene sequences.

## 4. Conclusions

The introduction of the low aeration stage was beneficial to the proliferation of denitrifying bacteria in the external anoxic zone of AGS, alleviating the competition for nutrients between heterotrophic aerobic microorganisms, nitrifying bacteria and denitrifying bacteria, increasing the ratio of AOB/NOB. Therefore, the short-range simultaneous nitrification and denitrification process could be achieved quickly. Moreover, two-stage aeration increased extracellular PN, which provided a basis for stability and good mass transfer of AGS.

Table 4

Shares of four genus in total bacteria Unit: %

Number	AOB	NOB	Paracoccus	Thauera	Denitrifying bacteria <sup>b</sup>	AOB/NOB
1	0.33	0.28	6.76	10.34	17.10	118
2	2.32	0.09	14.24	4.88	19.12	2577
3	2.13	0.46	8.59	5.13	13.72	463
2+3	4.45	0.55	22.83	10.01	32.84	809

<sup>b</sup>Share of denitrifying bacteria is the sum of Paracoccus and Thauera.



## Acknowledgments

This work was supported by water project of National Science and Technology Major Project (Grant No. 2015ZX07202-013).

## References

- [1] S.S. Adav, D.J. Lee, Extraction of extracellular polymeric substances from aerobic granule with compact interior structure, *J. Hazard. Mater.*, 154 (2008) 1120–1126.
- [2] M.K. de Kreuk, N. Kishida, M.C.M. van Loosdrecht, Aerobic granular sludge-state of the art, *Water Sci. Technol.*, 55 (2007) 75–81.
- [3] X.C. Quan, Y. Cen, F. Lu, L.Y. Gu, J.Y. Ma, Response of aerobic granular sludge to the long-term presence to nanosilver in sequencing batch reactors: reactor performance, sludge property, microbial activity and community, *Sci. Total Environ.*, 506 (2015) 226–233.
- [4] D. Gao, L. Liu, H. Liang, W.M. Wu, Aerobic granular sludge: characterization, mechanism of granulation and application to wastewater treatment, *Crit. Rev. Biotechnol.*, 31 (2011) 137–152.
- [5] S.S. Adav, L. Duujong, J.Y. Lai, Potential cause of aerobic granular sludge breakdown at high organic loading rates, *Appl. Microbiol. Biotechnol.*, 85 (2010) 1601.
- [6] Y.M. Lin, K.G.J. Nierop, E. Girbal-Neuhauser, M. Adriaanse, M.C.M. van Loosdrecht, Sustainable polysaccharide-based bio-material recovered from waste aerobic granular sludge as a surface coating material, *Sustain. Mater. Technol.*, 4 (2015) 24–29.
- [7] C. Caudan, A. Filali, M. Sperandio, E. Girbal-Neuhauser, Multiple EPS interactions involved in the cohesion and structure of aerobic granules, *Chemosphere*, 117 (2014) 262–270.
- [8] A. Mosquera-Corral, M.K. de Kreuk, J.J. Heijnen, M.C.M. van Loosdrecht, Effects of oxygen concentration on N-removal in an aerobic granular sludge reactor, *Water Res.*, 39 (2005) 2676–2686.
- [9] Y. Liu, J.H. Tay, State of the art of biogranulation technology for wastewater treatment, *Biotechnol. Adv.*, 22 (2004) 533–563.
- [10] J. Wan, M. Sperandio, Possible role of denitrification on aerobic granular sludge formation in sequencing batch reactor, *Chemosphere*, 75 (2009) 220–227.
- [11] J.B. Xavier, M.K. De Kreuk, C. Picioreanu, M.C.M. Van Loosdrecht, Multi-scale individual-based model of microbial and bioconversion dynamics in aerobic granular sludge, *Environ. Sci. Technol.*, 41 (2007) 6410–6417.
- [12] B.S. McSwain, R.L. Irvine, Dissolved oxygen as a key parameter to aerobic granule formation, *Water Sci. Technol.*, 58 (2008) 781–787.
- [13] J.H. Tay, Q.S. Liu, Y. Liu, The effect of upflow air velocity on the structure of aerobic granules cultivated in a sequencing batch reactor, *Water Sci. Technol.*, 49 (2004) 35–40.
- [14] APHA. Standard Methods for the Examination of Water and Wastewater. American Public Health Association, Washington, D.C. USA 1998.
- [15] Y. Aoi, T. Miyoshi, T. Okamoto, S. Tsuneda, A. Hirata, A. Kitayama, T. Nagamune, Microbial ecology of nitrifying bacteria in wastewater treatment process examined by fluorescence in situ hybridization, *J. Biosci. Bioeng.*, 90 (2000) 234–240.
- [16] X. Wang, M. Ji, J. Wang, Z. Yang, Study on the extraction of extracellular polymer from aerobic granular sludge, *China Water Wastewater.*, 21 (2005) 91–93.
- [17] X. Zhao, Z. Chen, X. Wang, J. Li, J. Shen, H. Xu. Remediation of pharmaceuticals and personal care products using an aerobic granular sludge sequencing bioreactor and microbial community profiling using Solexa sequencing technology analysis, *Bioresour. Technol.*, 179 (2015) 104–112.
- [18] Z.X. Ning, Food Composition Analysis Manual. China light industry press, Beijing, 1998.
- [19] B. Frolund, R. Palmgren, K. Keiding, P.H. Nielsen, Extraction of extracellular polymers from activated sludge using a cation exchange resin, *Water Res.*, 30 (1996) 1749–1758.
- [20] J. Wan, Y. Bessiere, M. Sperandio, Alternating anoxic feast/aerobic famine condition for improving granular sludge formation in sequencing batch airlift reactor at reduced aeration rate, *Water Res.*, 43 (2009) 5097–5108.
- [21] X. Zhang, H. Zhang, C. Ye, M. Wei, J. Du, Effect of COD/N ratio on nitrogen removal and microbial communities of CANON process in membrane bioreactors, *Bioresour. Technol.*, 189 (2015) 302–308.
- [22] V. Poot, M. Hoekstra, M.A. Geleijnse, M.C van Loosdrecht, J. Perez, Effects of the residual ammonium concentration on NOB repression during partial nitrification with granular sludge, *Water Res.*, 106 (2016) 518–530.
- [23] B. Wookkeun, B.E. Rittmann, A Structured model of dual-limitation kinetics, *Biotechnol. Bioeng.*, 49 (1996) 683–689.
- [24] L. Wu, C. Peng, S. Zhang, Nitrogen removal via nitrite from municipal landfill leachate, *J. Environ. Sci. (China)*, 21 (2009) 1480–1485.
- [25] L. Samuel, G.G. Graciela, H. Christof, Optimized aeration strategies for nitrogen and phosphorus removal with aerobic granular sludge, *Water Res.*, 47 (2013) 6187–6197.
- [26] J.E. Schmidt, B.K. Ahring, Granular sludge formation in upflow anaerobic sludge blanket (UASB) reactors, *Biotechnol. Bioeng.*, 49 (1996) 229–246.
- [27] T. Seviour, M. Pijuan, T. Nicholson, J. Keller, Z.G. Yuan, Gel-forming exopolysaccharides explain basic differences between structures of aerobic sludge granules and floccular sludges, *Water Res.*, 43 (2009) 4469–4478.
- [28] L.W. Hulshoff Pol, S.I. de Castro Lopes, G. Lettinga, Anaerobic sludge granulation, *Water Res.*, 38 (2004) 1376–1389.
- [29] C. Wang, B. Xie, L. Han, X. Xu, Study of anaerobic ammonium oxidation bacterial community in the aged refuse bioreactor with 16S rRNA gene library technique, *Bioresour. Technol.*, 145 (2013) 65–70.
- [30] W. Bian, S.Y. Zhang, Y.Z. Zhang, W.J. Li, R.Z. Kan, W.X. Wang, Z.M. Zheng, J. Li, Achieving nitrification in a continuous moving bed biofilm reactor at different temperatures through ratio control, *Bioresour. Technol.*, 226 (2017) 73–79.
- [31] K.R. Hartop, M.J. Sullivan, G. Giannopoulos, A.J. Gates, P.L. Bond, Z. Yuan, T.A. Clarke, G. Rowley, D.J. Richardson, The metabolic impact of extracellular nitrite on aerobic metabolism of *Paracoccus denitrificans*, *Water Res.*, 113 (2017) 207.
- [32] L. Yan, S. Zhang, G. Hao, X. Zhang, Y. Ren, Y. Wen, Y. Guo, Y. Zhang, Simultaneous nitrification and denitrification by EPSs in aerobic granular sludge enhanced nitrogen removal of ammonium-nitrogen-rich wastewater, *Bioresour. Technol.*, 202 (2016) 101.